Characterization of Hot Deformation of CW602N Brass

S. Spigarelli*, M. El Mehtedi and M. Cabibbo

DIISM, Università Politecnica delle Marche, via Brecce Bianche 60131 Ancona, Italy

Alpha brasses (in principle single-phase solid solution alloys containing less than 35% Zn) are usually processed by extrusion, forging or rolling. Although these materials are of widespread use, few detailed studies of the flow behavior of brass at high temperature are available. The hot workability of a CW602N brass (Cu–36.5%Zn–2%Pb) was thus investigated by torsion testing in the temperature range between 550 and 800 °C, under equivalent strain rates ranging from 0.01 to 10 s^{-1}. The peak flow stress dependence on temperature and strain rate was described by the well-known Garofalo equation, with a stress exponent close to 4 and Q =220 kJ mol^{-1}. A considerably larger scatter of the experimental data was observed in the high temperature range. The detailed microstructural analysis of the deformed samples by scanning electron microscopy revealed substantial differences among the samples deformed in the low temperature regime and those torsioned at 750 and 800 °C. These differences were analyzed and discussed to rationalize the different mechanical responses observed in the two hot-deformation regimes.

1. Introduction

The recent introduction of finite element modelling (FEM) codes to simulate hot working processes (see, for an example, [1]), has highlighted the need for quantifying the mechanical response of the involved material, in term of constitutive equations relating strain, strain rate, temperature and flow stress. The high temperature deformation of single-phase α-brass has been considered in several studies [2–5], which analyzed in most cases the creep response of the Cu–30%Zn alloy [2–4]. Among the most recent publications, only in one case [5] the hot workability of Cu–30%Zn was investigated by torsion testing. In this study, the flow stress (σ) was related to strain rate ($\dot{\varepsilon}$) and temperature (T) by the well-known Garofalo equation,

$$\alpha\dot{\varepsilon} = A\left[\sinh\left(\alpha'\sigma\right)\right]^{n}\exp\left(-Q/RT\right), \qquad (1a)$$

where α' [MPa^{-1}] and A [s^{-1})] are material parameters, R is the gas constant, n is the stress exponent and Q is the activation energy for hot working. Equation (1a) was here rewritten in the form

$$\dot{\varepsilon} = A\left[\sinh\left(\alpha\sigma/G\right)\right]^{n}\exp\left(-Q/RT\right), \qquad (1b)$$

where G is the elastic modulus in shear, α, now dimensionless, is again a material parameter. Pernis and co-workers [5] obtained for the Cu–30%Zn, n =4.3 and Q =180 kJ/mol. Not surprisingly, these values are very close to those calculated by Raj [4] by analyzing the creep response of a similar material (n =4.1–5.4 and Q =175 kJ/mol).

The increase in Zn content leads to the formation of the bcc β' ordered phase, which at high temperature evolves in the disordered bcc β solid solution; the resulting $\alpha-\beta$ microstructure of the Cu–40%Zn brass, at working temperatures, even undergoes superplastic

_____

*corresponding author; e-mail: s.spigarelli@univpm.it

deformation [6–9], due to extensive grain boundary sliding along the α/β interfaces [10, 11]. An analysis of the peak flow stress data presented by Xiao et al. [12] in their investigation of the hot workability of a Cu–38%Zn shows that, in this $\alpha-\beta$ brass, the stress exponent is slightly lower than in Cu–30%Zn (n =3.9), while the activation energy is substantially higher (Q =257 kJ/mol). Similar values (n =3.9, Q =222 kJ/mol) can be obtained by fitting the data presented by Padmavardhani and Prasad [13] for a Zn–39.5%Zn–3%Pb brass. Although one can reasonably wonder if Pb could play a role in determining the material response, the presence of this alloying element, which is liquid at the hot-working temperature, was shown to not affect the Arrhenius plots used for the calculation of the activation energy [14]. For this reason, any effect of Pb addition in leaded brasses is usually neglected.

A further increase of the Zn-content above 40% causes the progressive decrease of the volume fraction of α-phase, until, for a Cu–44%Zn, the microstructure is composed entirely by β-phase. The use of Eq. (1) to interpolate the peak flow stresses obtained in [13] by testing in compression a Cu–44%Zn, results in n = 3, and $Q \approx$ 100 kJ/mol. It is thus plainly obvious that the magnitudes of the stress exponent and of the activation energy for hot working strongly depend on the initial microstructure of the considered brass. While n seems to monotonically decrease with increase of the Zn content, Q is relatively high for pure copper (201 kJ/mol, activation energy for self-diffusion) [2], decreases down to 175 kJ/mol for 30%Zn [4], then increases up to 250 kJ/mol and above, to again decrease down to 100 kJ/mol when the Zn content is sufficiently high to produce a single-phase β-microstructure.

In this context, the aim of the present study is to analyze the hot workability of a Cu–36.5%Zn–2Pb leaded brass, in order to establish the constitutive equation relating flow stress and deformation conditions.

2. Experimental

The alloy considered in the present study was the CW602N brass (Cu–36.5%Zn–2%Pb–As, composition in wt%). The material was tested in torsion; the hot torsion test is capable of producing strains of the order of 100 in ductile materials without the instabilities which cause barrelling and necking in compression and tension, respectively. When the shear stresses and strains obtained in torsion are converted into equivalent tensile stresses and strains, for example according to the von Mises criterion, torsion flow curves agree very well to tension or compression flow curves for the same strain rate and temperature. For this reason, the torque M and the number of revolutions N were converted to von Mises equivalent stress σ and equivalent strain ε at the surface

$$\sigma = \frac{\sqrt{3}M}{2\pi r^3}\left(3 + n' + m'\right), \tag{2a}$$

$$\varepsilon = \frac{2\pi N r}{\sqrt{3}L}, \tag{2b}$$

where r and L are, respectively, the radius and the length of the gauge, $m' = \left(\partial \log M / \log \dot{N}\right)$ is determined at constant strain, and $n' = \left(\log M / \partial \log N\right)$ at constant strain rate. For the peak stress condition, clearly $n' = 0$. For the sake of simplicity, m' (which was estimated to be 0.15 and 0.23 at 550 and 700 °C, respectively) was also assumed to be equal to 0, leading to an underestimation of the flow stress which not exceeded 8%. The surface equivalent strain rates were 10^{-2}, 10^{-1}, 1 and 10 s^{-1}. The specimens for torsion tests, 10 mm in diameter with a gauge length of 15 mm, were strained, by a computer-controlled hot torsion machine at 550, 600, 650, 700, 750 and 800 °C. The samples were heated by a high frequency induction coil at 1 °C/s from room temperature to the testing temperature and maintained at this temperature for 300 s. Subsequently the samples were strained up to rupture. Ruptured samples were quenched by a water-jet.

Samples for scanning electron microscopy were obtained from the as received alloy and from the outer portion of the torsioned specimens. Standard grinding and polishing metallographic techniques were used to prepare the samples for etching with Nital (nitric acid in distilled water).

3. Results and discussion

Figure 1a shows representative equivalent stress vs. equivalent strain curves. In general, the curves present a maximum, for strains ranging between 0.7 and 1.2; the equivalent strain to fracture, presented in Fig. 1b, decreases with increasing strain rate. The lowest values are observed at 550 °C; no dependence of the strain to fracture on temperature was then observed between 600 and 700 °C. Above this temperature range, the equivalent strain to fracture in torsion exhibits a significant increase with temperature. The analysis of Fig. 1b thus seems to
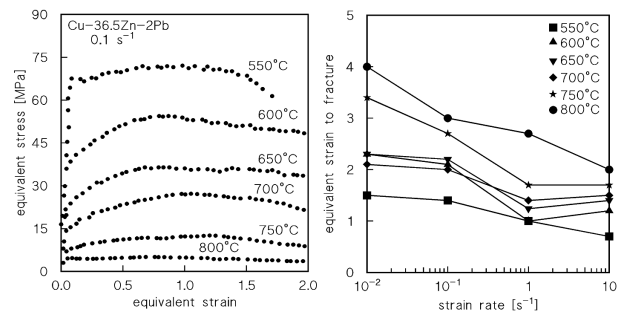

Fig. 1. a) Representative equivalent stress vs. equivalent strain curves in torsion; (b) equivalent fracture strain as a function of testing temperature and strain rate.
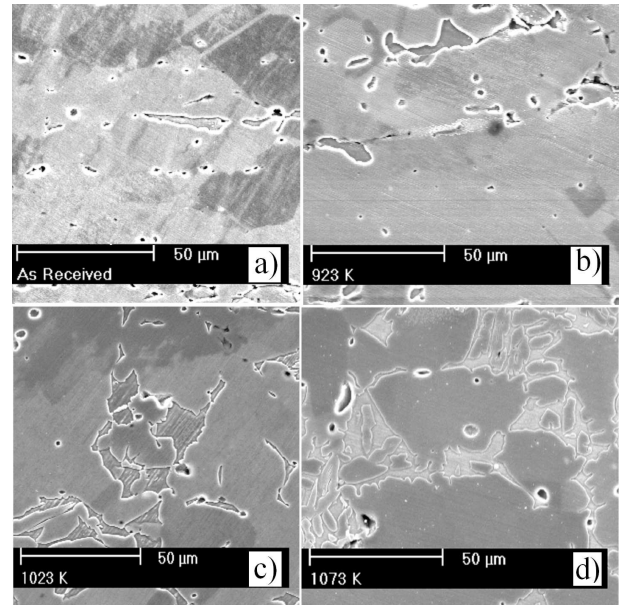

Fig. 2. Microstructure in as received condition (a) and after torsion under 0.01 s^{-1}: (b) 650 °C (strain = 2.2); (c) 750 °C (strain = 3.4); (d) 800 °C (strain = 4.0). The α-grains constitute the grey matrix, while the particles on grain boundaries are β/β' bcc phase.

suggest that at 750 and 800 °C the microstructure undergoes an important change that significantly increases the ductility of the alloy.

Figure 2 shows the microstructure of the as received alloy, and after straining at 650, 750 and 800 °C. Figure 2a clearly shows the presence in as received condition of a minor but not negligible amount of β or β' phase (the elongated particles in the matrix of α-grains). Although heating up to 650 °C causes only a moderate increase in the presence of the bcc phase, at 750 and 800 °C massive blocks of β appear at the grain boundaries.

Figure 3 shows the Cu–Zn phase diagram [15]; the experimental conditions used to test the hot workability of different brasses are superimposed on the graph. In can be easily observed that, in equilibrium conditions, while in the case of the Cu–40%Zn, the alloy is two-phase in the
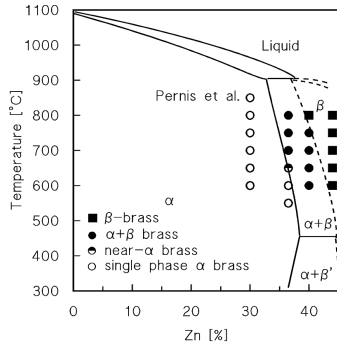
Fig. 3. Cu–Zn phase diagram [15]; symbols represent the testing temperature investigated in this study, and in literature for Cu–30%Zn [5], Cu–40%Zn [13] and 44%Zn, respectively [13].
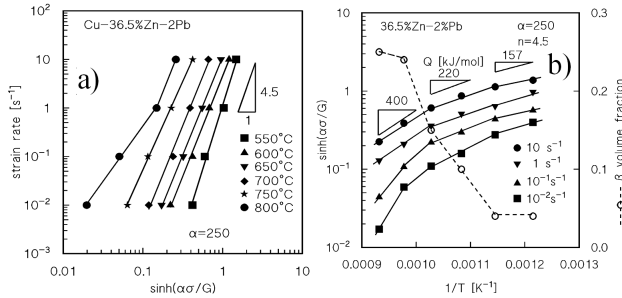

Fig. 4. Peak flow stress dependence on strain rate as a function of temperature (a) and plot used for the calculation of the hot deformation activation energy; the graph also illustrates the volume fraction of β phase as measured in the sample torsioned at 0.01 s^{-1} (b).

whole range between 550 and 750 °C, the Cu–36.5%Zn brass of the present study, has a single phase microstructure below 700 °C, while becomes two-phase above this temperature. The presence of either β or β'-phase at room temperature, attested in Fig. 2a, and confirmed in the literature for similar alloys [16], is thus presumably the effect of non-equilibrium transformations during material processing.

Figure 4a plots the peak flow stress as a function of strain rate for the investigated alloy; the figure shows that, with α =250, a reasonably constant slope of the curves is obtained between 550 and 750 °C, with n =4.5. A different behavior is observed at 800 °C, in particular in the low strain rate regime, where a significantly lower stress exponent is obtained.

The activation energy for high deformation is usually calculated by plotting the sinh$(\alpha\sigma/G)$ as a function of $1/T$ (Fig. 4b); in principle the data, as long as the activation energy is constant, should align on straight lines of slope S, where

$$Q = 2.3nRS. \tag{3}$$

In the present case, the data rather align on curves whose slope markedly increases with increase of temperature. In the low temperature regime, where the β-content is lower, the apparent activation energy is close to 157 kJ/mol.

This value is fully consistent with those estimated in Cu–30%Zn in [4, 5] (175–180 kJ/mol), since both Q_{Zn}^* and Q_{Cu}^* (activation energy for tracer diffusion of Zn and Cu in brass, respectively) decrease with increase of Zn content [17]. Equation (1) can be rewritten [4] as

$$\dot{\varepsilon} = A_0 \tilde{D} \left[\sinh\left(\alpha\sigma/G\right) \right]^n, \tag{4}$$

where $\tilde{D}$ is the complex diffusion coefficient for dislocation climb, which, following Fuentes-Samaniego and Nix [18, 19], can be expressed as a function of the atomic fraction of Cu and Zn (N_{Cu} and N_{Zn}) in the form

$$\tilde{D} = \tilde{D}_0 \exp\left(-Q_c/RT\right) =$$

$$\left(N_{Cu}D_{Cu}^* + N_{Zn}D_{Zn}^*\right)/0.78 \tag{5}$$

with

$$D_{Cu}^* = D_{0Cu}^* \exp\left(-Q_{Cu}^*/RT\right), \tag{6a}$$

$$D_{Zn}^* = D_{0Zn}^* \exp\left(-Q_{Zn}^*/RT\right). \tag{6b}$$

Since, according to Anusavice and DeHoff, also the diffusion constants D_{0Zn}^* and D_{0Cu}^* decrease with increase of the Zn content above 20%, the complex diffusion coefficient for climb can be expected to monotonically decrease in this composition range. Thus, the activation energy for climb, Q_c, should be well below 175 kJ/mol when Zn = 36.5%.

As temperature rises, the increase in volume fraction of the softer bcc phase causes the marked softening of the alloy. The higher the β-amount, the softer the material becomes, leading to a progressive curvature of the log(sinh$(\alpha\sigma/G)$) vs. $1/T$ plot. This effect, in turns, leads to progressively higher Q-values when the activation energy is calculated by Eq. (3). Thus, this Q value can be more correctly identified as an apparent activation energy, since it does not depend only on the diffusivities of the alloy, but is greatly affected by the presence of a softer phase, whose amount in turn depends on temperature. If the whole temperature range above 550 up to 700 °C is considered, an average value of the apparent activation energy of 220 kJ/mol can be estimated. This value is fully consistent with those, above mentioned, for $\alpha-\beta$ alloy, which is not surprising, since at 650–700 °C the alloy contains 10–15% of β-phase.

Figure 5a shows the Zener–Hollomon parameter $Z = \dot{\varepsilon}\exp\left(Q/RT\right)$, with Q = 220 kJ/mol; as expected , almost all the experimental data quite closely align on a same straight line of slope $n = 4.5$, except the low-strain rate results at 750 and 800 °C. The low strength observed in these conditions corresponds to the high values of equivalent strain to fracture shown in Fig. 1b, and both these phenomena can be attributed to the increased presence of β-phase.

The above qualitative discussion on the effect of the increased presence of a soft-phase (the β-phase) in a hard-matrix (the α-phase), clearly suggests that the material of the present study could be efficaciously described by the composite model based on the rule of mixtures. Thus, the material strength can be calculated as
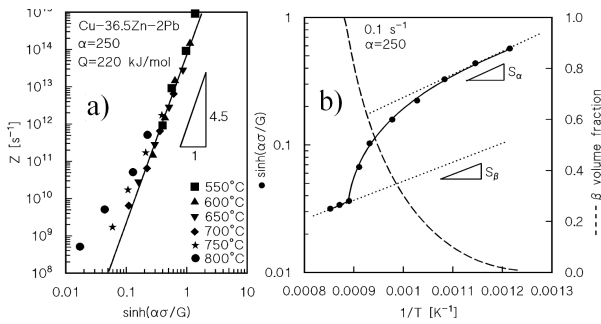
Fig. 5. Zener–Hollomon parameter as a function of peak flow stress (a) and same plot of Fig. 4b at 0.1 s^{-1}, for the alloy of the present study, containing the equilibrium volume fraction of β-phase (broken line in the graph), whose strength was recalculated by the composite model (b). The S_α and S_β slope give, through Eq. (3), $Q = 157$ and 92 kJ/mol, respectively.

$$\sigma = (1 - f_s)\,\sigma_h + f_s\sigma_s, \tag{7}$$

where the suffixes s and h denote the soft and hard regions, respectively, and f_s is the volume fraction of the soft β-phase [20]. According to Fig. 3 an alloy containing 36.5%Zn (corresponding to a Cu/Zn ratio close to 1.68, which, translated into a binary alloy composition, corresponds to Cu–37.2%Zn) could be described by a composite formed by hard α-phase with 36%Zn, and a soft β-phase with 42–44%Zn. Each phase obeys a constitutive equation in the form of Eq. (1), with $\alpha = 350$, $n = 3$, $Q = 92$ kJ/mol and $A = 1.44 \times 10^7$ s^{-1} for the soft phase (Zn = 44%), and $\alpha = 250$, $n = 4.5$, $Q = 157$ kJ/mol and $A = 6.6 \times 10^9$ s^{-1} for the hard phase (Zn = 36%) (see Ref. [20] for a detailed discussion on the calculation of these parameters). Combination of these data with Eq. (7), for an alloy containing the equilibrium volume fraction of β-phase, gives the plot presented in Fig. 5b (with $\alpha = 250$). The analogy between Figs. 4b and 5b is self-apparent, thus attesting that the non-monotonic value of the apparent activation energy for hot working is an artefact due to the presence of a composite-like microstructure.

4. Conclusions

The hot workability of a Cu–36.5%Zn–2Pb brass was investigated by torsion testing between 550 and 800 °C. Two different regimes were identified: (i) a low temperature regime (550–700 °C), where the volume fraction of soft β-phase remained below 15%, the stress exponent in the Garofalo equation was close to $n = 4.5$, the average value of the apparent activation energy for deformation was close to 220 kJ/mol, and the equivalent strain to fracture was relatively low; (ii) a high temperature regime (750–800 °C), characterized by higher volumes of soft β-phase, by very high values of the apparent activation energy for hot working (300–400 kJ/mol) and by high values of the equivalent strain to fracture.

The differences in hot workability, as well as the anomalous dependence of the apparent activation energy for hot-working, are considered to be effects of the microstructural instability, which leads to the formation of higher amounts of β-phase as temperature is increased above 650 °C.

References

[1] J.R. Cho, H.S. Jeong, D.J. Cha, W.B. Bae, J.W. Lee, *J. Mater. Proc. Tech.* **160**, 1 (2005).

[2] R.M. Bonesteel, O.D. Sherby, 0.1016/0001-6160(66)90096-4*Acta Metall.* 14, 385 (1966).

[3] S.A. Mahmoud, M.A. Semary, Z.M. Farid, N. El-Naquib, *Mater. Sci. Eng. A* **118**, 107 (1989).

[4] S.V. Raj, *J. Mater. Sci.* **26**, 3533 (1991).

[5] R. Pernis, J. Kasala, J. Boruta, *Kovove Mater.* **48**, 41 (2010).

[6] M. Suery, B. Baudelet, *J. Mater. Sci.* **8**, 363 (1973).

[7] J.W.D. Patterson, N. Ridley, *J. Mater. Sci.* **16**, 457 (1981).

[8] D. Hua, W. Qingling, M. Lonxiang, *J. Mater. Sci.* **27**, 607 (1992).

[9] K. Neishi, Z. Horita, T.G. Langdon, *Scr. Mater.* **45**, 965 (2001).

[10] T. Chandra, J.J. Jonas, D.M.R. Taplin, *J. Mater. Sci.* **13**, 2380 (1978).

[11] H. Miyamoto, T. Tanaka, T. Mimaki, R. Matsubara, N. Ashie, S. Miura, *Mater. Sci. Eng. A* **380**, 34 (2004).

[12] Y.-H. Xiao, C. Guo, X.-Y. Guo, *Mater. Sci. Eng. A* **528**, 6510 (2011).

[13] D. Padmavardhani, Y.V.R.K. Prasad, *Metall. Trans.* **22A**, 2993 (1991).

[14] B.L. Vaandrager, G.M. Pharr, *Scr. Metall.* **18**, 1337 (1984).

[15] A.P. Miodownik, in: *ASM Handbook*, Vol. 3, 1987, p. 2.

[16] V. Buršiková, J. Buršik, V. Navrátil, K. Milička, *Mater. Sci. Eng. A* **324**, 235 (2002).

[17] K.J. Anusavice, R.T. DeHoff, *Metall. Trans.* **3**, 1279 (1972).

[18] R. Fuentes-Samaniego, W.D. Nix, *Scr. Metall.* **15**, 15 (1981).

[19] R. Fuentes-Samaniego, W.D. Nix, G.M. Pound, *Acta Metall.* **29**, 487 (1981).

[20] S. Spigarelli, M. El Mehtedi, M. Cabibbo, F. Gabrielli, D. Ciccarelli, *Mater. Sci. Eng. A* **615**, 331 (2014).